Important 2′-Hydroxyl Groups within the Core of a Group I Intron†

Mark G. Caprara and Richard B. Waring*

Department of Biology, Temple University, Philadelphia, Pennsylvania 19122

Received August 27, 1992; Revised Manuscript Received December 23, 1992

ABSTRACT: The catalytic activity of a group I intron is dependent on a core structure, much of which is not exposed to solvent. In order to study the structure of the core, an efficient bimolecular reaction has been developed: the 5′-component is a molecule of about 300 bases which contains the 5′-splice-site and terminates in the loop established by P8, and the 3′-component is a 24 base long oligoribonucleotide which includes the 3′-regions of the P8 and P7 helices with their joining region, J8/7. J8/7 is thought to play several roles including binding the helix containing the 5′-splice-site. P7 forms a major portion of the guanosine binding site required for splicing. We have modified the bimolecular system to make it amenable to kinetic analysis and have used it to study the role of the ribose sugars in the oligomer. Multiple deoxyribonucleotide substitution in the J8/7 region completely blocked 5′-splice-site cleavage even though the K_d was only reduced about 5-fold. This supports the idea that the ribose phosphate backbone in J8/7 plays a key role in catalysis. Individual substitutions at G303 and A306 reduced the rate of catalysis 5–10-fold. The G303 substitution blocked GTP-independent hydrolysis of the 5′-splice-site. The region spanning the junction of P8 and J8/7 was also highly sensitive to multiple deoxyribonucleotide substitution; however, only in the case of C298 did an individual substitution have any effect on cleavage. Deoxyribonucleotide substitution in the 3′-section of P7 was less severe, although k_{cat}/K_m in low GTP was down 70-fold.

The group I intron in the pre-RNA of the large ribosomal subunit in *Tetrahymena thermophila* is a ribozyme able to catalyze its own excision and the ligation of its flanking exons (Cech et al., 1981). Identification of the important structural features of the intron is fundamental to understanding how this RNA can act as a catalyst. A secondary structure model of the intron based on phylogenetic comparison of known group I introns has been supported by mutational and biochemical modification experiments (reviewed in Cech (1988); Burke, 1988). Additionally, some tertiary interactions also predicted by phylogenetic comparisons have been supported by mutational analysis (Michel et al., 1990). These studies have established that there is a core of nucleotides encompassed by P3–P8 which is primarily responsible for catalytic activity (Figure 1A). Chemical probing has revealed that in the folded molecule much of the ribose phosphate backbone is buried, being protected from a solvent-based reagent (Latham & Cech, 1989). Using a phylogenetic data base and molecular modeling, Michel and Westhof (1990) have proposed a three-dimensional model for the conserved core of group I introns.

Chemical synthesis of short RNA molecules is now not only possible but also fairly routine (Usman et al., 1987). The enormous possibilities afforded by this technique include the introduction of site-specific chemically modified nucleotides within a particular RNA sequence. One significant modification that has been used successfully is replacement of the 2′-OH of the ribose sugar with an H-atom (Wu et al., 1989a). Natural DNA molecules have not been shown to have catalytic activity or even to contribute to a complex of nucleic acids having catalytic activity, indicating that the ribose groups play a key role in overall ribozyme function. Ribozymes can tolerate partial but not global substitution of ribose with deoxyribose and can be sensitive to substitution in key regions, particularly those thought to be single stranded (Perreault et al., 1991). Deoxyribonucleotide substitution has been used to explore the role of the ribose 2′-OH in binding the 5′-exon to the *Tetrahymena* intron (Pyle & Cech, 1991; Pyle et al., 1992; Bevilacqua & Turner, 1991).

We have developed a bimolecular system that splits the conserved core of the *Tetrahymena* intron and has one component short enough for chemical synthesis. Particular attention has been paid to making it amenable to kinetic analysis. We have focused on the P8–J8/7–P7 region for several reasons: (1) it is one of the two most highly conserved regions of the intron; (2) it is close to the guanosine binding site (Michel et al., 1989; Yarus et al., 1991); and (3) its ribose phosphate backbone is likely to be rich in tertiary interactions (Waring, 1989; Michel & Westhof, 1990; Pyle et al., 1992). We have used this system to study the effects of site-specific deoxyribonucleotide substitutions within the core of the intron and have identified three specific ribose groups with an influential role in RNA catalysis.

MATERIALS AND METHODS

Bimolecular Reaction. The basic design of the bimolecular system includes a precursor RNA (containing the 5′-splice-site) that is truncated at the loop of L8 and a complementary fragment that includes the 3′-P8 stem, the J8/7 sequence, and the 3′-P7 stem (Figure 1A). The following alterations were made to optimize the bimolecular system. Preliminary work using transcribed RNA indicated that the wild-type pyrimidine-rich sequence in the P8 region of a 3′-molecule could bind to the internal guide sequence of a bimolecular complex and inhibit the reaction at high concentrations. To avoid this problem, two A-U base pairs were replaced in P8 without reducing splicing activity (C283-G295, U284-A294, Figure 1A). An initial 5′-construct, ending in the sequence 5′-GAAUCG instead of 5′-GAUAGAU as in Figure 1A, underwent a cyclization reaction. Although it seems somewhat implausible, the size of the RNA generated is consistent with the 3′-end attacking the cyclization site of the intron at base

† This work was supported by NIH Grants GM 41009 to R.B.W. and SO RR07115.

* Author to whom correspondence should be addressed.

0006-2960/93/0432-3604$04.00/0

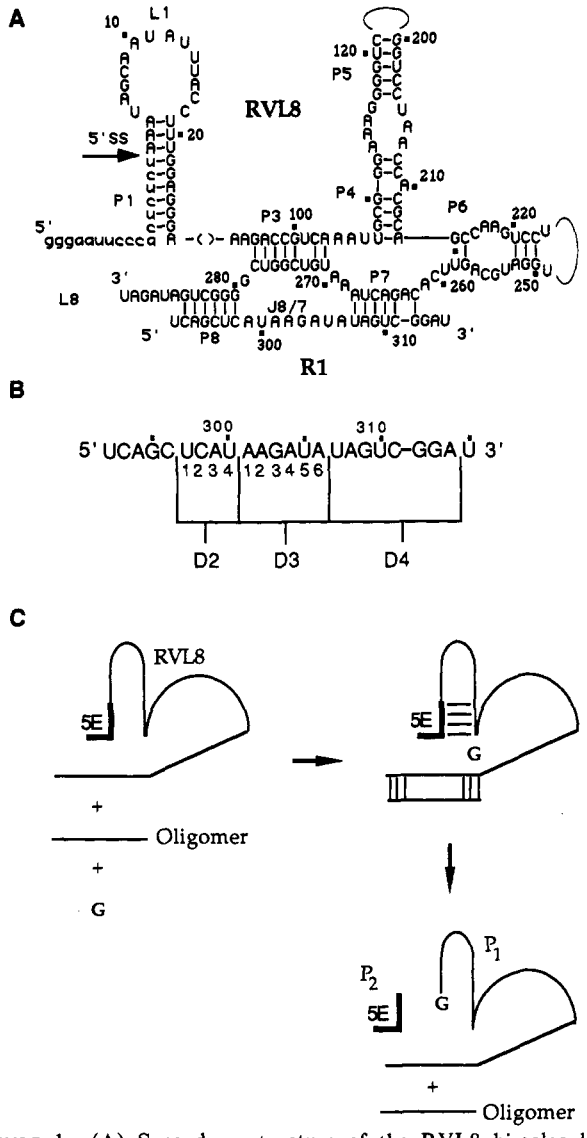

FIGURE 1: (A) Secondary structure of the RVL8 bimolecular construct. Portions of P5, P5a,b,c, and P6a and the whole of P2 and P2.1 have been left out for simplicity. The arrow points to the 5'-splice-site (5'SS), and lowercase lettering shows the 5'-exon bound to the internal guide sequence. (B) Position of deoxyribonucleotide substitution in the oligomers. Oligomers containing several contiguous substitutions are called D2, D3, and D4, and the regions they encompass are outlined. Singly substituted oligomers are numbered after their parent oligomer (see also Table I). (C) Proposed reaction pathway for the RVL8 system: G = exogenous GTP; P_1 = RVL8 minus the 5'-exon with GTP covalently attached to its 5'-end; P_2 = released 5'-exon.

15, as does the 3'-end of the intron during normal splicing (Tanner & Cech, 1987). Consistent with this possibility is the fact that the RNA ended in the sequence UCG, as does the normal intron, and our observation that if P8 is destabilized by the introduction of two base mismatches in P8 (C283-U295 and U284-U294), catalytic activity is still retained.

Oligonucleotides. The all RNA and mixed DNA/RNA polymers were synthesized by either National Biosciences (Plymouth, MN) (D2, D3, and D4) or Biopolymer Labs (Camden, NJ) (R1, D21–D24, and D31–D36). The oligonucleotides were deprotected following published protocols (Stawinski et al., 1988; Wu et al., 1989b). The deprotected oligonucleotides were purified by electrophoresis in 20% polyacrylamide (19:1 acrylamide/bis) and 7 M urea gels. The oligomers were located by UV shadowing, excised, and eluted overnight in 0.3 M sodium acetate, 20 mM Tris-HCl, pH 7.5, and 1 mM EDTA (ATE) at 4 °C. The oligomers were spun through a 0.45-μm membrane filter (Vanguard International), extracted with phenol/chloroform/isoamyl alcohol (25:24:1), precipitated with ethanol, passed through a Sephadex G-25 spun column, precipitated again, and dissolved in water. Concentrations were determined by absorption at 260 nm using a conversion factor 27.3 μg per OD unit. Each oligomer was 5'-end-labeled, and the sites of deoxyribonucleotide substitution were confirmed by partial hydrolysis degradation (100 mM NaOH, 3 min, 37 °C) followed by electrophoresis in a 20% polyacrylamide/7 M urea gel against a G specific sequence ladder generated by partial RNase T1 digestion (Donis-Keller et al., 1977). Dilutions of the polymers were routinely kept as dried pellets at -20 °C.

RVL8. The RVL8 construct was made by cassette mutagenesis (Sambrock et al., 1989) of the plasmid pTT14 (Waring, 1989). This mutation places an *Eco*RV restriction site at the start of the L8 loop, changes bases in the 5'-stem of P8 as described above, and deletes the entire intron sequence downstream of L8. After digestion with *Eco*RV and ethanol precipitation, RVL8 was prepared by transcription with T7 RNA polymerase (Waring, 1989) from this template. The RNA was purified from a 5.5% polyacrylamide/7 M urea gel essentially as for the oligonucleotides, except that the chromatography step was omitted. Concentrations were estimated at 260 nm using a factor of 40 μg per OD_{260} unit (Sambrock et al., 1989). Internally labeled RVL8 was prepared by inclusion of [α-^{32}P]GTP (NEN, 800 Ci/mmol) in the transcription mix.[1] This RNA was located by autoradiography of the preparative gel, and concentrations of the final purified product were determined by counting radioactivity.

Native Gel Analysis. Labeled or unlabeled RVL8 was routinely snap cooled by heating to 95 °C for 2 min, adding a 5× reaction buffer (see the Standard Cleavage Reactions section), and then placing the mixture on ice. Unlabeled or labeled oligomer was added to the RVL8 mix after separately preheating the solutions to 50 °C. After incubation for 15 min at 50 °C, the samples were placed at 4 °C and loaded onto a running 10% or 7% polyacrylamide gel (30:1 acrylamide/bis) containing 50 mM Tris/HOAC (pH 7.5) and 25 mM $Mg(OAC)_2$. The gels were run for 10–14 h at 4 °C at 8 W.

The dissociation constants of R1, D22, D33, and D36 were measured using this native gel system (see Pyle et al. (1990)). The concentration of labeled oligomer was kept at 20 nM, while that of unlabeled RVL8 ranged from 5 to 500 nM. After incubation of oligomer and RVL8 at 50 °C, the sample was cooled to 4 °C. This essentially freezes the reaction since the ratio of bound to free oligomer does not change for at least 2 h when the reaction is cooled in this way. When it is diluted 10-fold at the time of the temperature shift the ratio does not change, indicating that no disassociation of the oligomer occurs. No association occurs either since complex formation is not detected when the binding reaction is performed for 1 h at 4 °C (M. G. Caprara and R. B. Waring, unpublished data). The bound complexes were separated from free oligomers using the native gel system described above. The ratio of bound to free oligomer was determined by excising the appropriate bands from the gel and Cherenkov counting. For each oligomer, the experiment was repeated at least three times, and the data were analyzed using "k-cat" software (Biometallics Inc., Princeton, NJ).

Standard Cleavage Reactions. Snap-cooled, labeled RVL8 (50 nM) in the reaction buffer (final concentrations, 50 mM

[1] Abbreviations: GTP, guanosine triphosphate; G, guanosine; Tris, Tris(hydroxymethyl)aminomethane; EDTA, ethylenedinitrilotetraacetic acid disodium salt; OAC; acetate; 5'SS, 5'-splice-site.

Tris-HCl, pH 7.5, 100 mM $(NH_4)_2SO_4$, and 25 mM $MgCl_2$) was preincubated for 4 min at 30 or 50 °C and added to a 30 or 50 °C mix of oligomer (final concentration, 5 or 200 nM) and GTP (final concentration, 1 mM). The reactions were stopped after 60 min by addition of an equal volume of formamide stop buffer containing 95% formamide, 0.05% bromophenol blue, 0.05% xylene cyanol, and 50 mM EDTA and then analyzed by electrophoresis in 5.5% polyacrylamide/7 M urea gels.

Multiple Turnover Experiments. All time course measurements were determined at 50 °C in the above reaction buffer conditions with oligomer concentrations at 5 nM and a range of RVL8 concentrations (as indicated for each experiment). For reactions under low GTP conditions (2.5 μM final concentration), [α-^{32}P]GTP was used and RVL8 was unlabeled. When 1 mM GTP was used, labeled RVL8 was included in the reaction and the GTP was unlabeled. During each experiment the reactions were centrifuged every 5 min to minimize the effect of evaporation of the sample. The products of the reaction were quantitated either by scanning of the autoradiograms with an Ultroscan densitomer (Pharmacia) or by excising the labeled products from the gel and counting the amount of radioactivity.

Single Turnover Experiments. In the single turnover reactions, oligomers were present at 1 μM and RVL8 at 3 nM under standard buffer conditions. The appropriate oligomer was preincubated with snap-cooled RVL8 for 15 min at 50 °C before GTP was added to a final concentration of 1 mM or before the first time point was taken for single turnover reactions in the absence of GTP. Reactions were fractionated by gel electrophoresis and quantified by scanning the autoradiograms with an Ultroscan densitometer (Pharmacia). Reactions shorter than 7 s were performed by doing each time point separately in triplicate. Stop dye separated by an air space was included in the same pipet tip as the prebound RVL8–oligomer complex, which was then added to a small volume of GTP to initiate the reaction. After the appropriate time, the stop dye was injected. No reaction occurred if stop dye and sample were injected simultaneously.

RESULTS

RVL8 Bimolecular System. Normally splicing occurs by two transesterification reactions. First the 3′-hydroxyl of a free guanosine attacks the 5′-splice-site (5′SS), and then the 3′-hydroxyl of the released 5′-exon attacks the 3′-splice-site to generate ligated exons and the released intron (Cech, 1988). Bimolecular reactions consisting of transcripts terminating in L8 (Figure 1) combined with transcripts starting in L8 through to the 3′-exon are active in 5′- and 3′-splicing (M. G. Caprara and R. B. Waring, unpublished data). Sequences downstream of P7 are not required for cleavage of the 5′SS (Doudna et al., 1987; M. G. Caprara and R. B. Waring, unpublished data). We therefore designed a 3′-P8–J8/7–3′-P7 segment that would support catalysis and be a convenient size for chemical synthesis. An oligo*deoxy*ribonucleotide of 24 bases spanning this region did not act as an inhibitor of a bimolecular reaction involving transcribed RNAs, whereas a 28-mer with a 4-base extension of P8 did. We therefore reasoned that an oligoribonucleotide of the 24-mer (R1, Figure 1A) might give adequate, but reversible, binding. This was indeed the case, but several adjustments to the P8 sequence and the unpaired nucleotides of the 5′-molecule (RVL8, Figure 1A) had to be made to avoid side reactions and to optimize activity before the system was suitable for kinetic analysis (see Materials and Methods).

Pyle et al. (1990) developed a native gel system to monitor the formation of a bimolecular complex between the *Tetrahymena* ribozyme and a 5′-exon analogue. Using this assay, they determined which of the 5′-exon's 2′-OH groups contributed significantly toward binding to the ribozyme. We adapted this system to assay complex formation between RVL8 and R1 (Figure 2).

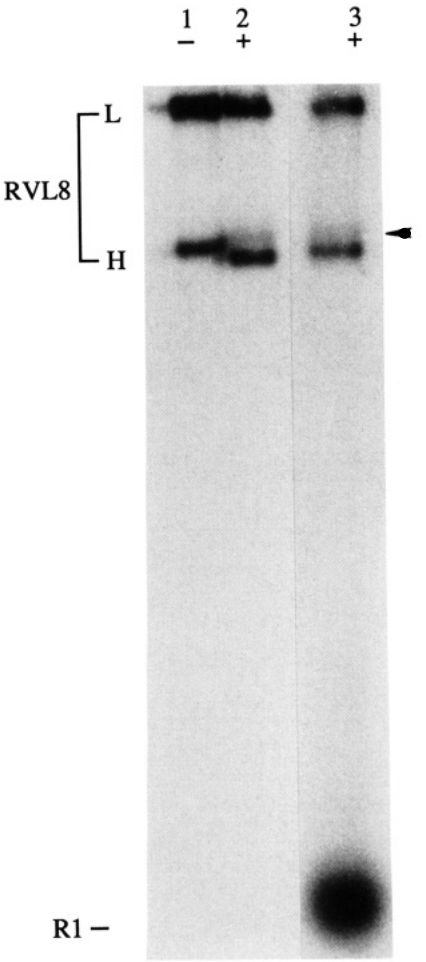

FIGURE 2: Native gel of the RVL8 and R1 complex. RVL8 preparations were not snap cooled. L and H indicate two RVL8 isomers resolvable in the gel system. Labeled RVL8 (50 nM) was incubated at 50 °C for 15 min without (–) or with (+) R1 (100 nM). In lane 3, ^{32}P-labeled R1 (20 nM) was incubated with unlabeled RVL8 (50 nM). The arrow indicates an alternative and slower form of the major bimolecular complex involving the RVL8 H isomer and R1—it is a very minor species at 50 °C.

RVL8, by itself, ran as two isomers (Figure 2, lane 1). When RVL8 at low concentrations (3–150 nM) was heated to 95 °C and quick cooled on ice in the presence of Mg^{2+} (snap-cooling), the amount of the low-mobility species was significantly reduced (data not shown). When the concentration of RVL8 was increased above ~175 nM, the low-mobility form predominated no matter how the RNA had been pretreated. This suggests that the low-mobility species is an intermolecular form of the high-mobility species.

When radioactively labeled RVL8 was incubated in the presence of a molar excess of unlabeled R1, a band appeared running just faster than the high-mobility form of RVL8 (Figure 2, lane 2). End-labeled R1 incubated with unlabeled RVL8 shifted R1 to a similar position on the gel, indicating that the band is a complex of R1 and RVL8 (Figure 2, lane 3). Some R1 also migrated with the low-mobility form of RVL8, indicating that it is also able to bind R1. We observed no difference in cleavage rates between snap-cooled and untreated preparations of RVL8 in multiple turnover experiments (50 nM RVL8, 5 nM R1 and see below) performed

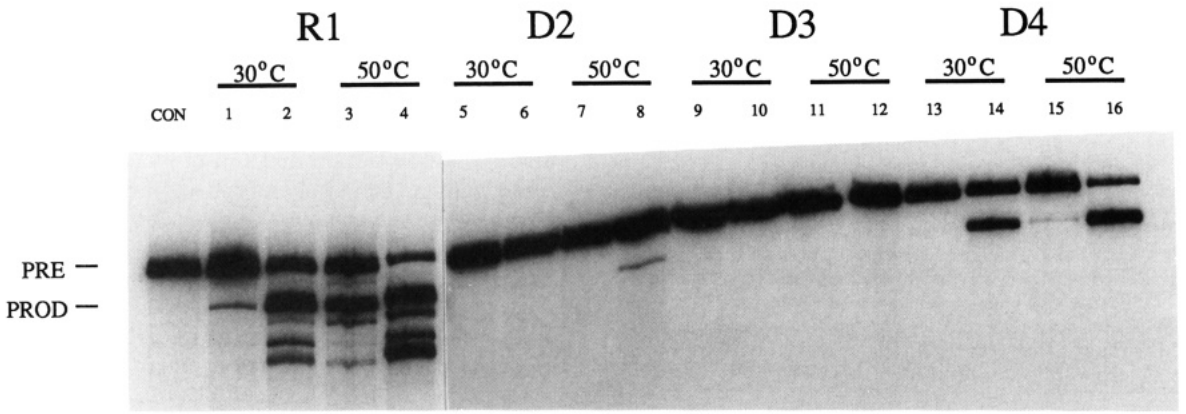

FIGURE 3: Effect of multiple deoxyribonucleotide substitution upon 5′SS cleavage efficiency. Reactions were carried out as described in Materials and Methods and contained 50 nM RVL8 with 5 nM oligomer (odd numbered lanes) or 200 nM oligomer (even numbered lanes): CON = RVL8 reacted without R1; PRE = uncleaved RVL8; PROD = RVL8 minus the 5′-exon (P_1 in Figure 1C). The additional product bands seen in the R1 lanes correspond to subsequent trans cleavage at bases 15 and 19 (Tanner & Cech, 1987) and an unidentified cryptic band that runs just below PROD, seen only during long incubation times in high GTP.

at 50 °C, suggesting that the two forms of RVL8 were at least kinetically similar.

The effects of Mg^{2+} concentration and temperature upon the cleavage reaction were investigated to determine suitable standard reaction conditions. An increase in the $MgCl_2$ concentration from 15 to 25 mM significantly increased the rate of the reaction. With R1 at 5 nM and RVL8 at 50 nM, only a stoichiometric amount of RVL8 was cleaved at 30 °C in 1 h, but at 50 °C 63% of the RVL8 substrate was cleaved, indicating that R1 was behaving catalytically and turning over at least 6-fold during the course of the reaction (Figure 1C). All subsequent reactions were performed in 25 mM $MgCl_2$ at 50 °C.

The bimolecular reaction may be described by the following reaction scheme:

$$S + E + G \underset{k_{-1}}{\overset{k_1}{\rightleftharpoons}} S{\cdot}E + G \underset{k_{-2}}{\overset{k_2}{\rightleftharpoons}} S{\cdot}E{\cdot}G \underset{k_{-3}}{\overset{k_3}{\rightleftharpoons}} G{-}P_1{\cdot}P_2{\cdot}E \xrightarrow{k_p^{off}} G{-}P_1 + P_2 + E \quad (1)$$

where the substrate (S) is RVL8 and the enzyme (E) is R1. P_1 is the cleaved intron fragment and P_2 the 5′-exon. The reaction is somewhat unorthodox in that the binding step describes the interaction of two components of the catalytic core of the enzyme, rather than the binding of the region of the RNA to be cleaved, which is the 5′SS in RVL8 (Figure 1C). Binding of G will depend on prior formation of the bimolecular complex (Yarus et al., 1991) as, presumably, will docking of the helix containing the 5′SS (Figure 1A,C) (Pyle et al., 1992; Hershlag, 1992).

Effects of Multiple Deoxyribonucleotide Substitution. Three analogues of R1 were synthesized, in which different regions of the oligomer were substituted with deoxyribonucleotides (Figure 1B). The cleavage reaction in 1 mM GTP was completely inhibited by substituting the J8/7 region (D3) with deoxyribonucleotides, significantly slowed (approximately 1% of the R1 activity) by substituting four nucleotides overlapping the P8–J8/7 junction (D2), and reduced by replacing the 3′-region of P7 (D4) (Figure 3). A 3′-truncated version of the excised intron can be cleaved at bases 15 and 19 by exogenous GTP (Tanner and Cech, 1987). This reaction was seen in the bimolecular reaction with R1 (Figure 3, lanes 2–4) but not with any of the modified oligomers. By performing a gel-shift binding assay at concentrations of RVL8 and oligomer which gave 50% binding of R1, we estimated that the relative binding efficiencies of D2 and D3 were down about 5-fold while D4 was similar to R1 (data not shown). Therefore, the inactivity of D3 is not caused by a failure to form a bimolecular complex. In contrast, the all deoxyribonucleotide version of the 24-mer failed to bind RVL8 under similar conditions. The activity assay and binding assay together imply that D2 and D3 are defective in both binding and catalysis.

Table I: Relative Initial Velocities of Deoxy-Substituted Oligomers in 2.5 μM GTP

oligomers	substitution position	v_{rel}[a]
R1		1
D21	U297	0.70
D22	C298	0.21
D23	A299	1.31
D24	U300	0.74
D31	A301	0.91
D32	A302	1.07
D33	G303	0.19
D34	A304	1.47
D35	U305	0.89
D36	A306	0.14
D2	U297–U300	0
D3	A301–A306	0
D4	U307–A314	0.014

[a] v_{rel} values were determined from the linear portion of plots of product formed versus time and then normalized to the all RNA control (R1). Each v_{rel} value is the average from two independent experiments.

Single Deoxyribonucleotide Substitution. Oligonucleotides with single deoxyribonucleotide substitutions in D2 and D3 were assayed under subsaturating substrate conditions and at low GTP (2.5 μM) with the expectation that any substitution that changed either RVL8 binding, GTP binding, or catalysis might be detected.

The initial velocities of the reactions involving each oligomer are presented in Table I. Oligomers D22, D33, and D36, with deoxyribonucleotide substitutions in C298, G303, and A306, respectively, reduced the rate 5–7-fold, relative to the all RNA control. Note also that D4 was down 70-fold and D2 was inactive under these conditions. The behavior of D22, D33, and D36 was pursued further.

Binding and Multiple Turnover Analysis. In order to determine the effects of D22, D33, and D36 upon binding affinity, the dissociation constants at 50 °C were determined using a gel-shift assay (Table II). The K_d of D22 increased nearly 2-fold, while that of D36 decreased nearly 4-fold. Possible reasons for the D36 decrease include the following. D36 could have a reduced rate of dissociation. If R1 itself has some secondary/tertiary structure, which needs to melt prior to binding, the deoxyribonucleotide substitution could

Table II: K_d and 2.5 μM GTP Kinetic Parameters

oligomer	K_d (nM)[a]	K_m (nM)[b]	k_{cat} (min^{-1})[b]	k_{cat}/K_m[b] ($\times 10^5$ M^{-1} min^{-1})
R1	49 (±19)	151 (±54)	0.158 (±0.022)	10.5
D22	94 (±29)	276 (±114)	0.033 (±0.006)	1.20
D33	34 (±16)	134 (±77)	0.042 (±0.009)	3.13
D36	13 (±4)	147 (±88)	0.023 (±0.006)	1.56

[a] K_d values were determined as described in Materials and Methods. Errors are expressed as the standard error of the derived value from a theoretical value arrived at by nonlinear regression analysis of the data using "k·cat" software. [b] Kinetic parameters were determined from two sets of initial velocity measurements using a range of RVL8 concentrations (25–500 nM). The data were averaged and plotted using "k·cat" software. The errors are expressed as for the K_d determinations.

Table III: Rate Constants in 1 mM GTP Multiple Turnover Reactions

oligomer	k_{obsd} (min^{-1})[a]	k_{cat}/K_m ($\times 10^6$ M^{-1} min^{-1})[b]
R1	0.041	8.2
D22	0.023	4.6
D33	0.003	0.6
D36	0.040	8.0

[a] Each k_{obsd} value is the average of two independent experiments. [b] In these reactions, the concentration of RVL8 was 8 nM, well below the estimated K_m of the all RNA oligomer control (~250 nM in 200 μM GTP, see text), and so the reaction is essentially first-order with respect to the substrate (RVL8) concentration (Segel, 1975). k_{obsd} was obtained from plots of the log of substrate remaining versus time. k_{cat}/K_m was calculated by dividing the k_{obsd} by the enzyme (oligomer) concentration (Segel, 1975).

have destabilized this structure and increased the rate of association of D36. The values of k_{cat}, K_m, and k_{cat}/K_m at low GTP were determined from initial velocity measurements of multiple turnover experiments using 5 nM oligomer (E), 25–500 nM RVL8 (S), and low GTP (2.5 μM). The results indicated that the substitutions were primarily affecting catalysis rather than substrate binding (Table II).

The rate of the cleavage reaction made it difficult to reliably determine these parameters at high GTP. Using conditions similar to those above but with 200 μM GTP, R1 was estimated to have values of K_m = 250 nM, k_{cat} = 1–3 min^{-1}, and k_{cat}/K_m = 4–12 M^{-1} min^{-1}. k_{cat}/K_m values at high GTP for the deoxyribonucleotide substitutions were obtained using pseudo-first-order reaction conditions with 5 nM E, 8 nM S, and 1 mM GTP (Table III). Under these conditions, only D33 showed a decrease in k_{cat}/K_m which represents the second-order rate constant for the reaction of free RVL8 and free oligomer. In order to focus on the catalytic steps subsequent to complex formation, single turnover experiments were conducted.

Single Turnover Analysis. Reactions were performed under substrate-saturating conditions at a saturating concentration of GTP with a prebinding step to ensure that complex formation was not a component of the reaction. Varying concentrations (0.01–2 μM) of R1 were prebound with 3 nM RVL8 to find the concentration that gave the maximal rate of cleavage upon addition of GTP. Rates of cleavage did not increase significantly when the concentration of R1 was raised above 250 nM. Therefore, a concentration of 1 μM was used for the single turnover reactions. This concentration should give 95% saturation of RVL8 on the basis of a K_d of 49 nM. Reactions performed without a prebinding step showed that GTP was close to saturation at 1 mM GTP since the reaction rates between 750 nM and 3 mM GTP were similar. We estimate the K_m for GTP in these conditions to be about 200–400 nM on the basis of a single series of experiments.

A time course of this reaction with 1 mM GTP revealed at least three phases (Figure 4). The last had an estimated rate constant of 0.047 min^{-1}, which was far slower than k_{cat} in multiple turnover conditions. The rate of the first and second were greater and comparable to k_{cat}, respectively. As the value of the K_d indicated that 95% of RVL8 was bound under these conditions, the last phase probably represented an inactive substrate–enzyme complex which, either slowly dissociated to eventually reassociate into an active complex, or slowly underwent a necessary conformational change prior to reacting. It was not permanently inactivated since >90% of the 3 nM RVL8 eventually reacted. After 15 min, all reactions, whether they involved R1 or modified oligomers, had accomplished the same amount of RVL8 cleavage (1.5 ± 0.1 nM) and were all proceeding at a similar slow rate. This implies that each reaction contained a similar fraction of active complex. This last, slow phase will be ignored in further discussions of the single turnover reactions.

In the R1 reaction the first and second phases were essentially over in under 10 s. The existence of the first phase burst was confirmed by measuring 1–7-s time points (Materials and Methods). The sizes and rates of the first and second phases obviously could not be measured accurately, but for comparative analysis, ranges were estimated. The first phase had a rate constant of >50 min^{-1} and presumably corresponds to a fraction of the bound complex undergoing a fast chemical step. The second phase had a rate constant of 3.5–8 min^{-1}, which is comparable to the value of k_{cat} (at 200 μM GTP) of 1–3 min^{-1}.

D22 was similar to but slightly slower than R1, although it was not examined over the first few seconds. D33 cleaved more slowly than R1 and no burst was detected. D36 cleaved more slowly than R1; the data suggested the presence of a small first phase burst (Figure 4), but its existence could not be conclusively determined due to its small size. The rate of the second (rate-determining) phase was lower than that of R1.

The 5′SS is subject to hydrolysis as well as cleavage by GTP (Inoue et al., 1986). Single turnover hydrolysis reactions at pH 7.5 were performed as described for GTP. D36 reduced the rate of hydrolysis 2-fold, while no activity was detected with D33 (Table IV).

DISCUSSION

Bimolecular System. We have begun the characterization of a bimolecular system designed to analyze the role played by a highly conserved region of the catalytic core of a group I intron. This region was provided as a 24-mer oligoribonucleotide. As preformed complexes reacted very rapidly (Figure 4), we conclude that the bimolecular system is a reasonable model of the unimolecular RNA. Native gel analysis showed that the RVL8 substrate existed in at least two forms at 50 °C (Figure 2, lane 1). Since the lower mobility form predominated at higher concentrations of RVL8, we assume that it is an intermolecular complex of RVL8, possibly a dimer formed by base-pairing between the 5′-terminal nucleotides in the 5′-exon (M. G Caprara and R. B. Waring, unpublished data). Both forms bound the R1 24-mer. There was no obvious difference between the reaction rate of the snap-cooled RVL8, which primarily consisted of the higher mobility form, and untreated RVL8, which primarily consisted of the lower mobility form.

Kinetic Description of the RVL8–R1 Bimolecular System. The observation that R1 could act catalytically prompted a description of the reaction pathway (see eq 1). A complete investigation of the individual rate constants within the

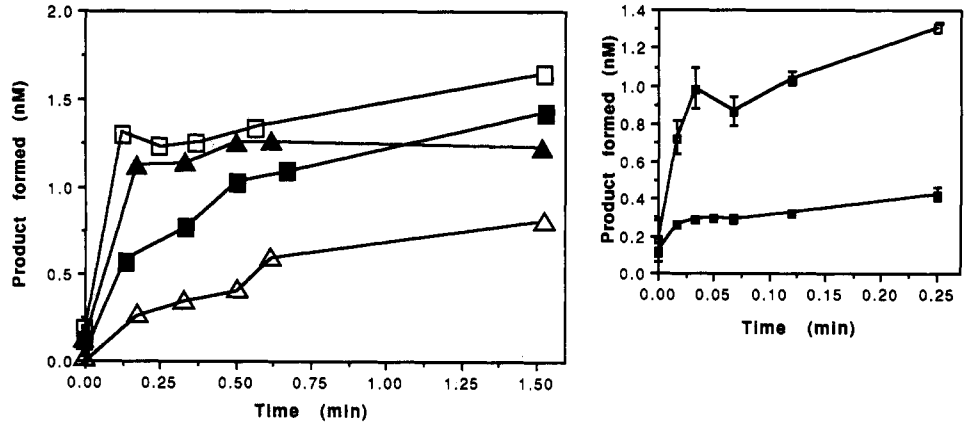

FIGURE 4: Product formed versus time plot for single turnover reactions in 1 mM GTP: R1 (□); D22 (▲); D33 (△); D36 (■). Similar profiles were obtained in two independent experiments. Inset: Plots for R1 and D36 showing the first 15 s of the reaction. Each time point for the first 7 s was performed in triplicate, and error bars are the standard deviation of the mean. Error bars for D36 are masked by the square symbol.

Table IV: Estimated Rate Constants for Single Turnover Reactions

	1 mM GTP			
oligomer	first phase k_{est} (min^{-1})	second phase k_{est} (min^{-1})	third phase k_{est} (min^{-1})[a]	hydrolysis k_{obsd} ($\times 10^{-3}$ min^{-1})[b]
R1	>50	8–3.5	0.048	6.0
D22	ND[d]	ND	0.12	3.9
D33		0.39	0.043	<0.001[c]
D36		1.2	0.037	3.0

[a] k_{est} for the third phase was determined by first plotting the log of the total substrate remaining (S_o = 3 nM) against time for the latter time points, and then the amount of substrate in this third phase (1.4 ± 0.1 nM) was estimated by extrapolating to t = 0. The second phase was analyzed by plotting the log of the substrate remaining in the 1st and 2nd phases (S_o = 1.6 nM) against time, and a range of the rate was estimated. Extrapolation to zero for R1 indicated that the 1st phase consisted of 0.4–0.7 nM (after subtracting material reacting during prebinding). This means that the rate of the 1st phase was >50 min^{-1}. [b] k_{obsd} for the hydrolysis reaction was obtained from first-order plots of the log of substrate remaining versus time. Each value is the average of two independent experiments. [c] No product was detected after 6 h of incubation. [d] ND = not determined.

pathway has not been completed, and so only limited information can be deduced from the multiple turnover analysis. However, the behavior of the single turnover reaction at 1 mM GTP with saturating, prebound R1 is consistent with a slow rate-limiting step occuring before a fast chemical step. The fast step had a rate constant of >50 min^{-1} (Table IV) and can be compared to the rate constant of about 350 min^{-1} for the chemical step in the system of Herschlag and Cech (1990). Throughout this work we consider the catalytic step to include all steps subsequent to complex formation and not just the chemical step. A slow step preceding chemistry can be described by an expanded version of the earlier reaction scheme:

$$E{\cdot}S \underset{k_{-x}}{\overset{k_x}{\rightleftharpoons}} E{\cdot}S' \xrightarrow{k_3} E{\cdot}P \qquad (2)$$

where E·S is an inactive form of the active E·S′ complex. The single turnover reaction (Figure 4) can be interpreted as follows. During preincubation, E·S and E·S′ reach their equilibrium concentrations. Addition of GTP leads to a very rapid conversion of E·S′ to E·P. The amplitude of the first phase burst would indicate that k_{-x} is approximately equal to k_x. The second phase would then represent the conversion of E·S to product. The value of the rate constant for this second phase (3–8 min^{-1}; see Table IV) is, as would be predicted, greater than or equal to the value of k_{cat} in a multiple turnover reaction at 1 mM GTP.

Effects of Deoxyribonucleotide Substitution in the P8–J8/7–P7 Region. The multiple deoxyribonucleotide substitutions that were made in the 24-mer oligoribonucleotide primarily affected the catalytic step of 5′SS cleavage rather than complex formation, since the rates of the cleavage reaction decreased far more than the values of the dissociation constant.

A reduction in 5′SS cleavage activity as a consequence of substitution of single deoxyribonucleotides in the region of nucleotides 297–306 was only clearly detected at positions C298, G303, and A306. Consistent with the effect of multiple substitutions, we observed in several ways that the single substitutions primarily affect steps subsequent to binding. First, k_{cat} was reduced for all three single substitutions under multiple turnover conditions at low concentrations of GTP (Table II). Second, deoxyribonucleotide substitution at either position G303 or A306 led to a marked change in the reaction profile of the single turnover experiment designed to study steps subsequent to binding (Figure 4); it was not possible to determine unambiguously how the two primary phases (1 and 2) were individually affected by these substitutions. Third, hydrolysis of the 5′SS was not detected when nucleotide G303 was substituted. This situation is similar to that found in the hammerhead ribozyme system where Perreault et al. (1991) observed that single deoxyribonucleotide substitutions within the ribozyme primarily affected k_{cat}.

Although deoxyribonucleotide substitution at position C298 led to a 5-fold drop in k_{cat} in 2.5 μM GTP (Table II), no striking change was seen in the single turnover experiment performed in 1 mM GTP. Substitution at C298 may therefore have an indirect effect on GTP binding.

No significant changes in the value of K_m were observed. Our preliminary screen (see Table I) was essentially for those substitutions which altered the value of K_m/k_{cat} at low concentrations of GTP. It is possible that we overlooked some substitutions with minor effects because of the potential reversibility of the cleavage reaction. In a normal enzyme-catalyzed cleavage reaction, one or both products dissociate much more rapidly from the active site than the substrate, thus preempting the reverse reaction (see also the bimolecular ribozyme system of Herschlag and Cech (1990)). In our system, the reverse reaction could be significant because GTP does not cleave the region of the substrate (RVL8) that is bound to the enzyme (R1) (Figure 1). This means that during the initial screening of the singly substituted oligonucleotides,

at a low concentration of GTP[2] under k_{cat}/K_m conditions (subsaturating RVL8), we may have missed effects on binding: substitutions that may have destabilized RVL8 binding (increasing K_m) could also have increased k_{cat} by reducing the extent of the reverse reaction through increasing the rate of product release.

Structural Roles of Identified Ribose Groups. The crystallographic analysis of yeast $tRNA^{Phe}$ revealed the dramatic potential for hydrogen bonding between a ribose 2′-OH group and either a donor or acceptor group (Quigley & Rich, 1976). However, impairment of function caused by deoxyribonucleotide substitution may not always be due to loss of a hydrogen bond. There are significant steric differences in the structures of polymers of single- and double-stranded RNA and DNA and their hybrids (Saenger, 1984; Chou et al., 1989). The effect of substituting deoxyribonucleotides in the four bases, U297–U300 (D2), was severe. This region spans the junction of P8 and J8/7 and is complex for three reasons. Firstly, P3 and P8 probably stack forming a pseudoknot with their ends directly abutting, close to the bottom of the P2 stem (Kim & Cech 1987; Michel & Westhof, 1990). Secondly, the *Tetrahymena* intron has an extra base, U300, which although not normally found in other group I introns, is highly intolerant of base substitution, and thirdly, its P8 stem is likely to end with a G279-A299 base pair (Couture et al., 1990). A single deoxyribonucleotide substitution at C298 immediately adjacent to this G-A base pair impaired 5′SS cleavage. The G-A base pair may make this region particularly sensitive to ribose substitution.

Almost one-half of the ribose residues in nonhelical regions of $tRNA^{Phe}$ are involved in 2′-OH hydrogen-bonding interactions to either nonbridging oxygens of phosphates or electronegative or electropositive groups on the bases, especially where long-range interactions or sharp turns are present (Quigley & Rich, 1976). Three-dimensional models of the group I intron (Kim & Cech, 1987; Michel & Westhof, 1990) predict that the J8/7 region is involved in just such interactions. Experimental data have established that docking of the P1 helix with the catalytic core is assisted by the formation of a hydrogen bond between the A302 base and the 2′-OH of u-3 in the 5′-exon (Pyle et al., 1992). In the Michel/Westhof model, J8/7 runs approximately parallel and in the same direction as the 5′-exon, turns sharply back on itself, possibly at A304 (Wang & Cech, 1992), and then turns again at A306 to start P7 with U307.

We have now accumulated evidence that single deoxyribonucleotide substitutions at highly conserved bases G303 and A306 partially impair catalysis, while multiple substitution from A301 to A306 completely inhibits catalysis. The ribose sugars of G303 and A306 are close to the G binding site (Wang & Cech, 1992). We have also previously established that phosphate nonbridging oxygens at A302, U305, A306, and A308 are involved in splicing (Waring, 1989). It is evident from these results that the ribose phosphate backbone in the J8/7 region of the intron plays a vital role in ribozyme activity.

[2] Exogenous GTP should decrease the rate of the reverse reaction by competing for the G binding site with the GTP attached to the 5′-end of RVL8 during the forward reaction. The reverse reaction should be inconsequential when the concentration of GTP is above K_m^G as is the case for the single turnover reactions in 1 mM GTP. At a low concentration of GTP, slow product release could permit a significant level of the reverse reaction to occur, even if the reactions are performed under k_{cat}/K_m conditions (subsaturating RVL8) when recycling of the oligomer due to slow product release should not be rate-limiting.

ACKNOWLEDGMENT

We thank John Burke for providing a plasmid used in preliminary experiments and Bill Geese for help with photography.

REFERENCES

Bevilacqua, P. C., & Turner, D. H. (1991) *Biochemistry 30*, 10632–10640.

Burke, J. M. (1988) *Gene 73*, 273–294.

Cech, T. R. (1988) *Gene 73*, 259–271.

Cech, T. R., Zaug, A. J., & Grabowski, P. J. (1981) *Cell 27*, 487–496.

Chou, S.-H., Flynn, P., & Reid, B. (1989) *Biochemistry 28*, 2435–2443.

Cornish-Bowden, A. (1979) *Enzyme Kinetics*, Butterworths, London.

Couture, S., Ellington, A. D., Gerber, A. S., Cherry, J. M., Doudna, J. A., Green, R., Hanna, M., Pace, U., Rajagopal, J., & Szostak, J. W. (1990) *J. Mol. Biol. 215*, 345–358.

Donis-Keller, H., Maxam A. M., & Gilbert, W. (1977) *Nucleic Acids Res. 4*, 2527–2538.

Doudna, J. A., Gerber, A. S., Cherry, J. M., & Szostak, J. W. (1987) *Cold Spring Harbor Symp. Quant. Biol. 52*, 173–180.

Herschlag, D. (1992) *Biochemistry 31*, 1386–1399.

Herschlag, D., & Cech, T. R. (1990) *Biochemistry 29*, 10159–10171.

Inoue, T., Sullivan, F. X., & Cech, T. R. (1986) *J. Mol. Biol. 189*, 143–165.

Kim, S. H., & Cech, T. R. (1987) *Proc. Natl. Acad. Sci. U.S.A. 84*, 8788–8792.

Latham, J. A., & Cech, T. R. (1989) *Science 245*, 276–282.

Michel, F., & Westhof, E. (1990) *J. Mol. Biol. 216*, 585–610.

Michel, F., Hanna, M., Green, R., Bartel, D. P., & Szostak, J. W. (1989) *Nature 342*, 391–395.

Michel, F., Ellington, A. D., Couture, S., & Szostak, J. W. (1990) *Nature 347*, 578–580.

Perreault, J.-P., Labuda, D., Usman, N., Yang, J.-H., & Cedergren, R. (1991) *Biochemistry 30*, 4020–4025.

Pyle, A. M., & Cech, T. R. (1991) *Nature 350*, 628–631.

Pyle, A. M., McSwiggen, J. A., & Cech, T. R. (1990) *Proc. Natl. Acad. Sci. U.S.A. 87*, 8187–8191.

Pyle, A. M., Murphy, F. L., & Cech, T. R. (1992) *Nature 358*, 123–128.

Quigley, G. J., & Rich, A. (1976) *Science 194*, 796–806.

Saenger, W. (1984) *Principles of Nucleic Structure*, Springer-Verlag, New York.

Sambrook J., Fritsch E. F., & T. Maniatis, T. (1989) *Molecular cloning: a laboratory manual*, Cold Spring Harbor Laboratory Press, Cold Spring Harbor, NY.

Segel, I. (1975) *Enzyme Kinetics*, John Wiley & Sons, New York.

Stawinski, J., Stromberg, R., Thelin, M., & Westman, E. (1988) *Nucleic Acids Res. 16*, 9285–9298.

Tanner, N. K., & Cech, T. R. (1987) *Biochemistry 26*, 3330–3340.

Usman, N., Ogilive, K. K., Jiang, M.-Y., & Cedegren, R. J. (1989) *J. Am. Chem. Soc. 109*, 7845–7854.

Wang, J., & Cech, T. R. (1992) *Science 256*, 526–529.

Waring, R. B. (1989) *Nucleic Acids Res. 17*, 10281–10293.

Wu, T., Ogilive, K. K., Perreault, J.-P., & Cedegren, R. J. (1989a) *J. Am. Chem. Soc. 111*, 8531–8533.

Wu, T., Ogilivie, K. K., & Pon, R. T. (1989b) *Nucleic Acids Res. 17*, 3501–3517.

Yarus, M., Illangesekare, M., & Christian, E. (1991) *J. Mol. Biol. 222*, 995–1012.